International Journal of Information, Control and Computer Sciences
ISSN: 2517-9942
Vol:5, No:11, 2011

A Robust Wheel Slip Controller for a Hybrid Braking System

Martin Ringdorfer and Martin Horn, *Member, IEEE*

Abstract—A robust wheel slip controller for electric vehicles is introduced. The proposed wheel slip controller exploits the dynamics of electric traction drives and conventional hydraulic brakes for achieving maximum energy efficiency and driving safety. Due to the control of single wheel traction motors in combination with a hydraulic braking system, it can be shown, that energy recuperation and vehicle stability control can be realized simultaneously. The derivation of a sliding mode wheel slip controller accessing two drivetrain actuators is outlined and a comparison to a conventionally braked vehicle is shown by means of simulation.

Keywords—Wheel slip control, sliding mode control, vehicle dynamics.

I. Introduction

OUR society's demand for mobility and flexibility is growing steadily. As a consequence the number of vehicles and traffic participants increases monotonically. In addition improved safety and reduced emissions play a significant role in the development of modern cars. This motivates the design of electric vehicles (EVs) and the improvement of vehicle dynamics control systems, like e.g. the electronic stability control (ESC).

Especially EVs offer potentials for exploiting the performance of chassis- and drivetrain-actuators in order to develop new safety features. One such approach is the utilization of single wheel electric traction drives (EM) in an EV drivetrain. As shown exemplarily in Fig. 1, a conventional car using hydraulic brakes and an EV equipped with single wheel traction drives on the rear axle are shown. In order to keep the vehicle stable during a braking maneuvre, the tire forces F_x have to be adapted wheel-independently. Control algorithms which are executed in an electronic control unit (ECU) use the drivers inputs (e.g. drive/brake-pedal, steering wheel input) for changing the tire forces appropriately. In state-of-the-art ESC systems, only the brake actuators are used for attaining the goal of safe driving. In EVs, the traction drives can be used for changing this forces as well. The idea of restoring kinetic energy as well as controlling the wheel slip in case of a blocking wheel can be brought into one line.

The development of such a wheel slip controller requires a mathematical model as derived in section II. The design of the wheel slip controller is presented in section III. Section IV shows simulation results and section V outlines future activities.

Martin Ringdorfer is with the Institute for Smart System Technologies, Klagenfurt University, Klagenfurt am Wörthersee, AUSTRIA and with Magna Powertrain AG & Co KG, Lannach, AUSTRIA martin.ringdorfer@uni-klu.ac.at.

Martin Horn is with the Institute for Smart System Technologies, Klagenfurt University, Klagenfurt am Wörthersee, AUSTRIA martin.horn@uni-klu.ac.at.

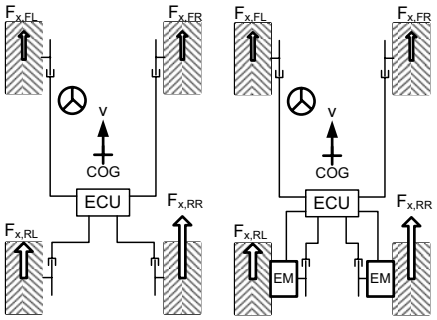

Fig. 1 Vehicle topology

II. Vehicle Model

The development of a wheel slip controller requires a detailed insight into the physical behaviour of the wheel assembly. For the description of the wheel dynamics, the quarter vehicle model, as depicted in Fig. 2, can be applied [3]. The introduced notation is summarized in table I.

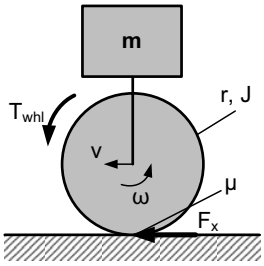

Fig. 2 Quarter vehicle model

Following the results of [5], the differential equation for the wheel slip λ reads as

$$\dot{\lambda} = \frac{r}{J \cdot v} \cdot T_{whl} - \frac{F_x \cdot r^2}{J \cdot v}. \tag{1}$$

According to [1] the tire force F_x reads as

$$F_x = F_{\max}(\mu) \cdot \sin\left(B(\mu) \cdot \left(1 - \mathrm{e}^{-\frac{|\lambda|}{A(\mu)}}\right) \cdot sgn(\lambda)\right) \tag{2}$$

where

$$A(\mu) = \frac{F_{\max}(\mu) \cdot B(\mu)}{c} \tag{3}$$

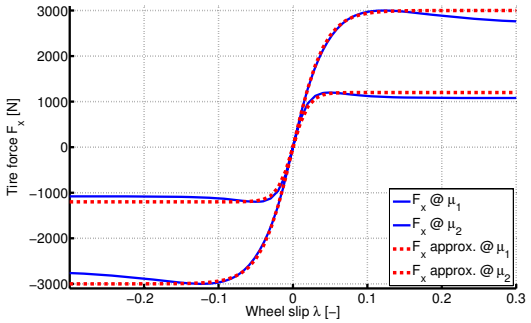

Fig. 3 Tire force approximation

TABLE I Quarter Vehicle Parameters

Identifier	Description	Unit
F_x	longitudinal tire force	N
F_∞	tire force at λ=1	N
F_{max}	maximum tire force	N
J	moment of inertia	kgm^2
T_{whl}	wheel torque	Nm
c	tire stiffness at λ=0	–
m	wheel load	kg
p_1, p_2, p_3, p_4	polynomial coefficients	–
r	dynamic tire radius	m
v	vehicle velocity	m/s
λ	wheel slip	–
μ	road surface friction coefficient	–
ω	angular tire velocity	rad/s

and

$$B(\mu) = \pi - \arcsin\left(\frac{F_\infty(\mu)}{F_{\max}(\mu)}\right). \tag{4}$$

Fig. 3 shows the tire forces F_x for different road surface friction coefficients μ. For the stable branch of the tire forces, the tire-characteristics can be approximated with sufficient accuracy using the polynomial

$$\begin{aligned} F_x(\mu,\lambda) &= F_{max}(\mu=1)\cdot\mu\cdot\ldots \\ &\ldots \cdot\tanh\left(\left(p_1\cdot\mu^3+p_2\cdot\mu^2+p_3\cdot\mu+p_4\right)\cdot\lambda\right). \end{aligned} \tag{5}$$

Using these results, it follows

$$\dot{\lambda}(\mu) = \frac{r}{J\cdot v}\cdot T_{whl} - \frac{F_x(\mu,\lambda)\cdot r^2}{J\cdot v}. \tag{6}$$

Equation (6) describes the wheel slip behaviour very satisfactory and therefore serves as a basis for the wheel slip controller design.

III. Controller Development

In EVs it is intended to recover as much electric energy as possible. For attaining this goal so-called "Operation strategies" (OPs) are applied. The task of the OP is to ensure efficient energy supply within the vehicle and maximizing the vehicles operation range. According to the state of charge of the electric energy storage system (ESS) and according to the drivers inputs, an optimal energy flow scenario is calculated. As a result of this evaluation, the determined electric torque T_E is applied to the motor controller. One possible schematic for such energy/control flow is shown in Fig. 4. With reference to table II, the motor produces the torque T_{EM}, which results in the wheel torque T_{whl}. During safe vehicle operation, only the OP calculates a wheel torque because the wheel slip controller is in its monitoring mode. While vehicle acceleration, the wheel torque reads as

$$T_{whl} = T_{EM}(T_E, T_\lambda = 0). \tag{7}$$

In case of a deceleration, the OP calculates a negative torque. If a negative T_E is applied, the traction motor operates as generator and the ESS is charged. In order to prevent the ESS from overcharging, the T_{EM} has to be limited. For ensuring a certain vehicle deceleration, a brake torque T_B can be applied additionally. This leads to T_{Brk} which is created by the hydraulic brake. The wheel torque follows as

$$T_{whl} = T_{EM}(T_E, T_\lambda = 0) + T_{Brk}(T_B, T_\lambda = 0). \tag{8}$$

The operation strategy torque T_{Op} results in

$$T_{Op} = T_B + T_E. \tag{9}$$

For μ-high conditions, the wheel slip controller is just monitoring the wheel dynamics. The wheel slip controller torque T_λ is zero. In case of slippery roads, the wheel torque T_{whl} potentially forces the tire to operate in its unstable region. The maximum possible force F_{max} is exceeded and the tire starts to skid. For preventing an unstable driving situation, a wheel slip controller has to limit the wheel torque by applying $T_\lambda \neq 0$.

$$T_{whl} = T_{EM}(T_E, T_\lambda) + T_{Brk}(T_B, T_\lambda) \tag{10}$$

In conventional cars an ESC is used for limiting the wheel torque during braking. This control system is only able to transform the kinetic energy of the vehicle into friction losses.

A. Equivalent Control

EVs provide the feature of using the kinetic energy for charging the ESS during vehicle deceleration. Therefore it is obvious, that the traction machines should operate as generators. Due to motor/ESS limitations, wheel slip control using EMs exclusively is only possible, if recuperation torques of certain amount are required. When these deceleration torques exceed the motors/ESS capabilities, a coordinated control of brake system and traction machines is inevitable. For analyzing the performance of coordinated control, PI-controllers for the EM and for the hydraulic brake were designed [6]. If both controllers operate in a "friendly coexistence", it can be seen from experiments, that the overall performance is poor. The benchmarked characteristics and the results can be seen in Fig. 6. As a conclusion from [5], an alternative control loop (see Fig. 4) was chosen. One PI-controller generates the reference values T_λ for the traction motor and the hydraulic brakes. Due to the different actuator dynamics [5] the performance can be improved significantly.

But still, there is potential for improvements. From equation (6) it is obvious, that the road friction surface coefficient has a wide influence on the plant dynamics. Therefore a special

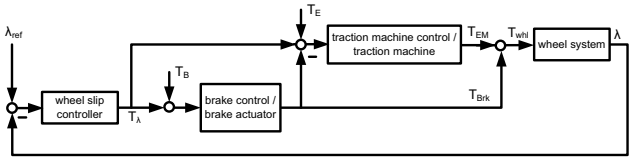

Fig. 4 Control loop

controller parameterization according to each possible μ/v-combination would lead to an optimum control behaviour. Having the knowledge about the actual μ-value would ease the problem of designing a slip controller. Unfortunately it is not possible to estimate μ with reasonable effort. In principle the amount of the applied wheel torque (with respect to wheel acceleration) gives a hint, whether the vehicle moves on μ-low or μ-high (11), as

$$\dot{\omega} = \dot{\omega}(\mu, \dot{T}_{whl}) \rightarrow \mu \approx \mu(\dot{\omega}, \dot{T}_{whl}). \tag{11}$$

Unfortunately, the exact values of the time-variant parameters p_1 - p_4 in equation (5) are not known. This means, that it is not possible to calculate $F_x(\mu, \lambda)$ accurately. Nevertheless, investigations revealed, that the application of sliding mode concepts is advantageous if the parameters μ and p_1 - p_4 are uncertain.

In the following, it is assumed, that

$$T_\lambda = T_{SMC} \tag{12}$$

holds.

Following the explanations from [7] and [2], the sliding mode controller output is chosen as

$$T_{SMC} = T_{eq} + T_{sw}. \tag{13}$$

If the OP applies its torque T_{Op} and under the assumption that the actuator dynamics are much faster than the wheel dynamics, it can be concluded from (6) that

$$\dot{\lambda} = -\frac{F_x(\mu, \lambda) \cdot r^2}{J \cdot v} + \frac{r}{J \cdot v} \cdot T_{Op} + \frac{r}{J \cdot v} \cdot T_{SMC}. \tag{14}$$

Let

$$\tilde{\lambda} = \lambda - \lambda_{ref} \tag{15}$$

be the tracking error of the wheel slip λ. By defining a sliding surface s as

$$s = \left(\frac{d}{dt} + \gamma\right) \cdot \int \tilde{\lambda} dt, \tag{16}$$

the time-derivate $\dot{s}$ can be computed as

$$\dot{s} = \dot{\tilde{\lambda}} + \gamma \cdot \tilde{\lambda}. \tag{17}$$

In case of a constant reference value λ_{ref} it results in

$$\dot{s}(\dot{\lambda}_{ref} = 0) = \dot{\lambda} + \gamma \cdot \tilde{\lambda}. \tag{18}$$

The sliding condition

$$\frac{1}{2} \cdot \frac{d}{dt} s^2 \leq \; k \cdot |s| \tag{19}$$

renders the sliding surface $s \equiv 0$ invariant.

The equivalent torque T_{eq} can be determined as

$$T_{eq}(\mu, \lambda, v) = \left(\frac{F_x(\mu, \lambda) \cdot r^2}{J \cdot v} - \gamma \cdot \tilde{\lambda}\right) \cdot \frac{J \cdot v}{r} - T_{Op}. \tag{20}$$

B. Discontinuous Control

For the equivalent control component, a "good" estimation of the mentioned polynomial parameters is required. As shown in Fig. 5 the required wheel torque T_{eq} can be calculated as a function of λ and v for a certain $\hat{\mu}$ and for an appropriate choice of p_1 - p_4. For an interval $\mu_{min} \leq \mu \leq \mu_{max}$, the same calculation can be accomplished. Preferably $\hat{\mu}$ is chosen as

$$\hat{\mu} = \frac{\mu_{min} + \mu_{max}}{2}. \tag{21}$$

It can be seen, that the required wheel torque increases with respect to velocity. According to the tire force characteristics in Fig. 3 the required torque increase with λ as well. Comparing the absolute distances between the calculated torque T_{eq} and the torques T_{whl} for the μ-boundaries, it can be seen, that they vary also. The shown torque distances represent the uncertainties which might occure, if the controller is designed for one special $\hat{\mu}$ while the existing μ differs from $\hat{\mu}$. In order to cope with these uncertainties, an additional discontinous torque

$$T_{sw} = -k \cdot sgn(s), k > 0 \tag{22}$$

is introduced.

The switching control law (22) is based on ideal actuator dynamics and leads to a very high switching frequency. This is a major drawback of sliding mode control, as its application leads to chattering. This phenomenon can be reduced by modifying the control law (22) according to

$$T_{sw} = -k \cdot sat\left(\frac{s}{\phi}\right), k > 0. \tag{23}$$

If k is chosen sufficiently large, it can be shown, that equation (19) is fulfilled [7]. Using the findings from Fig. 5, k is selected as

$$\begin{aligned} k &= k(\mu = \hat{\mu}, \lambda, v) \\ &= max(|T_{eq}(\hat{\mu}, \lambda, v) - T_{whl}(\mu_{min}, \lambda, v)|, ... \\ &\quad ...|T_{eq}(\hat{\mu}, \lambda, v) - T_{whl}(\mu_{max}, \lambda, v)|) + \epsilon. \end{aligned} \tag{24}$$

Extensive controller tests on different road friction surfaces revealed, that the computation of k should be changed according to

$$k = k\left(v, T_{Op}\right). \tag{25}$$

This is obvious because the controller operates around the tire force maximum F_{max}, where the uncertainties are highest. Additionally it reduces the controller tuning efforts.

The final control law results in

$$T_{sw} = -k\left(v, T_{Op}\right) \cdot sat\left(\frac{s}{\phi}\right). \tag{26}$$

Using a time-varying weighting parameter

$$\gamma = \gamma\left(\lambda - \lambda_{ref}\right) \tag{27}$$

TABLE II Controller Parameters

Identifier	Description	Unit
T_{Brk}	hydraulic brake torque	Nm
T_{EM}	traction motor torque	Nm
T_{Op}	operation strategy torque	Nm
T_E	operation strategy drive torque (EM-share)	Nm
T_B	operation strategy drive torque (brake-share)	Nm
T_{SMC}	sliding mode controller torque	Nm
T_{eq}	equivalent torque	Nm
T_p	pre-controller torque	Nm
T_λ	wheel slip controller torque	Nm
T_{sw}	switching torque	Nm
ϵ	additional switching torque amplitude	Nm
γ	weighting parameter	–
k	maximum amplitude of switching torque	Nm
$\hat{\mu}$	reference μ for equivalent control	–
ϕ	boundary layer width	–
p_{Brk}	brake pressure	bar
s	sliding surface	–
λ_{ref}	reference wheel slip	–
$\tilde{\lambda}$	tracking error	–

in equation (20) improves the control behaviour, with respect to the converging speed. Especially for μ-changes (e.g. μ-jumps) during wheel slip control action this technique is very effective.

C. Pre-Control

Due to limitations in the sampling frequency of the tire velocity ω and due to sensor noise, the feasible ranges of γ, ϕ and ϵ are limited. To overcome these limits, the introduction of a pre-control algorithm

$$T_p = T_p(\dot{\omega}, v) \tag{28}$$

is proposed.

D. Sliding Mode Control

The output of the wheel slip controller T_λ finally results as a linear combination of "equivalent control", "discontinous control" and "pre-control", i. e.

$$T_\lambda = T_{eq} + T_{sw} + T_p. \tag{29}$$

For reasons of unknown μ, the equivalent control component is calculated for a pre-defined $\hat{\mu}$ as

$$T_{eq}(\lambda, v) = \left(\frac{F_x(\hat{\mu}, \lambda) \cdot r^2}{J \cdot v} - \gamma \cdot \tilde{\lambda} \right) \cdot \frac{J \cdot v}{r} - T_{Op}. \tag{30}$$

IV. Simulation Results

For displaying the effectiveness of the proposed wheel slip controller, a comparison between a wheel slip controller accessing conventional brakes (see Fig. 1 left hand side) and the sliding mode hybrid controller (see Fig. 1 right hand side) was carried out. All simulations are based on a nonlinear 2-track model. Exemplarily a deceleration with Anti-Blocking-System-intervention (ABS-intervention) on μ-low is shown in Figs. 7-10.

- Conventional ABS: Front axle and rear axle are equipped with a hydraulic braking system.

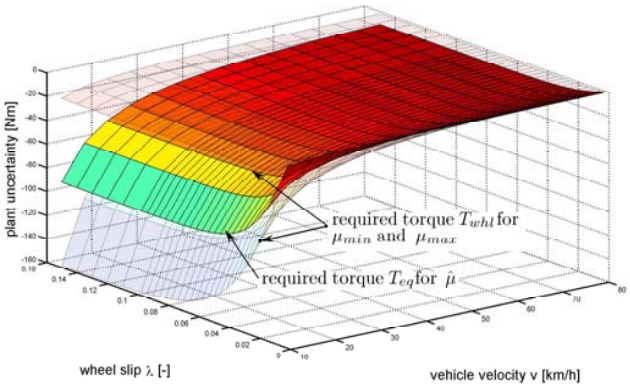

Fig. 5: Model Uncertainties

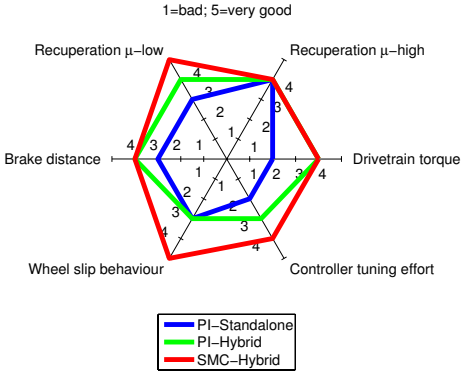

Fig. 6 Controller rating

- Hybrid ABS: The front axle is equipped with a hydraulic braking system. The rear axle is equipped with a "Hybrid"-braking system (traction motor and hydraulic brake) for maintaining wheel slip control and recuperation concurrently.

Conventional brake According to the drivers brake pedal input, a brake pressure is set up. Due to the limited brake force potential, the wheel starts to block. In order to keep the braking force on a high level, the ABS reduces the brake pressures, see Fig. 7. The brake pressures on the rear axle are smaller than on the front axle, in order to prevent the vehicle from oversteering. The wheel slip is adjusted as shown in Fig. 9. Fig. 10 reflects the deceleration of the wheels and the vehicle.

Hybrid brake According to the drivers brake pedal input and the ESS state of charge, a reference value for brake actuator and traction motor is computed by the OP. The reference values for the front axle are the same as in the conventional braking case. Instead of braking the rear axle by means of friction braking, a combination of recuperative braking and friction braking is applied, see Figs. 7-8. In case of exceeding the reference value λ_{ref}, the brake pressure and the traction motor torque are reduced by the wheel slip controller. From Fig. 9 it can be concluded, that the sliding mode controller stabilizes λ in a good way, although the dynamics of (1) varies in a remarkable range. The vehicle deceleration is depicted in Fig. 10.

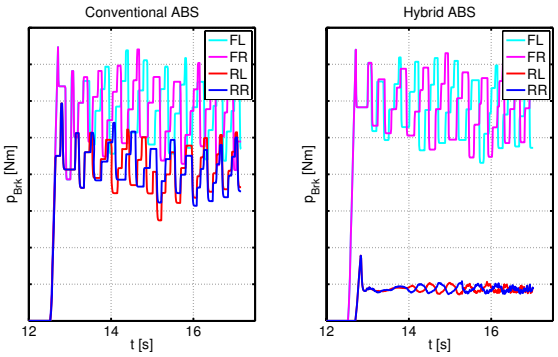

Fig. 7 Brake pressures

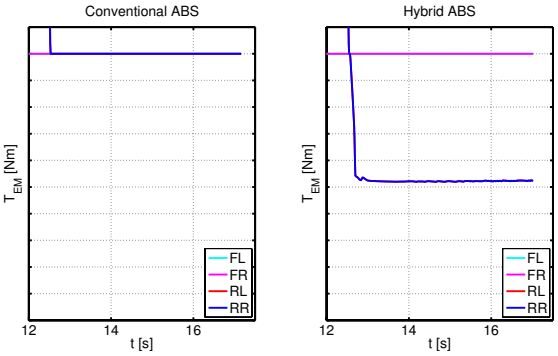

Fig. 8 Traction motor torques

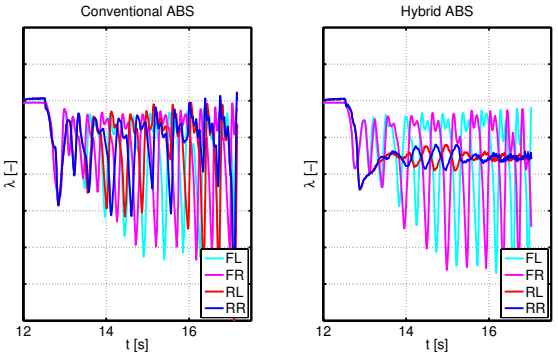

Fig. 9 Wheel slips

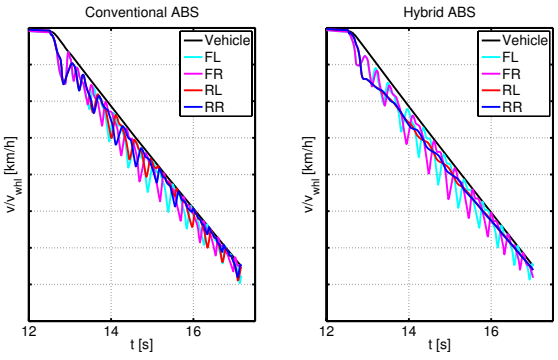

Fig. 10 Wheel velocities

V. Conclusion and Future Work

The present paper outlines the design of a wheel slip controller for an EV. Due to the time-varying behaviour of the plant and due to the model uncertainties, the application of a sliding mode controller is proposed. Based on a quarter vehicle model and on tire force approximation technique the equivalent control component is derived. Estimating the worst case model-uncertainties is helpful for finding the discontinuous controller component. Based on simulations, some further improvements of the controller performance were achieved. Finally, a comparison to a state-of-the-art controller confirms, that wheel slip control using electric traction machines and recovering electric energy do not exclude each other.

Future steps in the research project is the adaptation of the controller to different traction motor types and brake systems like e.g. electro-hydraulic brakes (EHB).

Acknowledgment

The authors gratefully acknowledge the support of the “Austrian Research Promotion Agency (FFG)” and “Magna Projecthouse Europe”.

References

[1] Hirschberg, W., “TM simple 4.0: A Simple to Use Tyre Model”, Graz University of Technology, 2008.
[2] Horn, M., et al., “Sliding-Mode Regelung von elektrischen Drosselklappen”, International Journal Automation Austria, 2008.
[3] Mitschke, M. et al., “Dynamik der Kraftfahrzeuge”, Springer-Verlag Berlin, 4.Auflage, 2004.
[4] Ringdorfer, M. et al., “Vehicle Dynamics Controller Concept for Electric Vehicles”, Proc. of AVEC10, 2010.
[5] Ringdorfer, M. et al., “Development of a Wheel Slip Actuator Controller for Electric Vehicles using Energy Recuperation and Hydraulic Brake Control”, Proc. of IEEE MSC2011, 2011.
[6] Sastry, S., “Nonlinear Systems”, Springer-Verlag Berlin, 1999.
[7] Slotine, L. et al., “Applied Nonlinear Control”, Prentice Hall, 1991.

Martin Ringdorfer studied Electronic Engineering at the University of Applied Sciences FH-Joanneum in Kapfenberg, where he graduated in 2005. Since that he has focused on different chassis and drivetrain control systems. Since 2009 he is working at the Institute for Smart System Technologies, Klagenfurt University, where he concentrates on vehicle dynamics controllers for electric vehicles.

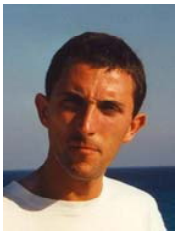

Martin Horn received the Dipl.-Ing. and the Ph.D. in electrical engineering from Graz University of Technology, Graz, Austria, in 1992 and 1998, respectively. Until 2008 he was with the Institute of Automation and Control at Graz University of Technology, Graz, Austria. In 2008 he joined the Alpen-Adria University Klagenfurt, Klagenfurt, Austria where he is currently a Professor for Control and Measurement Systems in the Institute for Smart System Technologies. His research interests are in the fields of variable structure systems, modeling and control of mechatronic systems and automotive control systems.